Journal of Fluids and Structures (2000) **14,** 1035–1051
doi: 10.1006/jfls.2000.0310, available online at http://www.idealibrary.com on IDEAL®

RESONANCES IN WAVE DIFFRACTION/RADIATION FOR ARRAYS OF ELASTICALLY CONNECTED CYLINDERS

T. UTSUNOMIYA
Department of Civil Engineering, Kyoto University
Kyoto, 606-8501, Japan

AND

R. EATOCK TAYLOR
Department of Engineering Science, University of Oxford
Oxford, OX1 3PJ, U.K.

(Received 20 January 1999, and in final form 12 May 2000)

As shown by Maniar & Newman in 1997, for a long array of bottom-mounted cylinders in the open sea, resonant modes occur as "near-trapping" and large diffraction forces are excited on the cylinders. The mechanism of such a resonant phenomenon was subsequently explained by the present authors in connection with the Dirichlet trapped modes for an array of cylinders aligned perpendicular to the walls in a wave channel. This paper examines similar resonant phenomena for radiation problems. Considered is an array of elastically connected cylinders in a wave channel. The cylinders are surface-piercing and extend to the sea-bottom. They constitute an array in a line, and each cylinder is allowed to oscillate only in the direction parallel to the line. Nonradiating wave modes, which cause only added mass force and no hydrodynamic damping are demonstrated to exist for an array of cylinders across the wave channel. Each mode corresponds to a "dry-mode" for the periodic array of elastically connected cylinders. This result leads to the existence of pure-resonant modes for a periodic array of elastically connected cylinders across the channel. Trapped modes for the corresponding diffraction problem are obtained as the limiting case when the stiffness of the springs has an infinite value.

1. INTRODUCTION

A TRAPPED MODE IS A RESONANT MODE in which only finite wave energy is trapped around an object/objects placed in an unbounded domain and no dissipation of wave energy due to radiation occurs [see Ursell (1951), Callan, Linton & Evans (1991), Evans & Kuznetsov (1998)]. Mathematically speaking, trapped modes are eigensolutions of the Laplace operator in an unbounded domain, in which only homogeneous boundary conditions are applied (that is, no forcing term). At the frequencies at which the trapped mode exists, uniqueness of the solution for the boundary value problem, in which inhomogeneous boundary conditions are applied on some boundaries, will be violated. Searching for trapped modes in many situations is thus a fundamental scientific problem, because in order to assure uniqueness of the solution for a diffraction/radiation problem we need to know whether the corresponding homogeneous problem has trapped-mode solutions or not.

0889–9746/00/101035 + 17 $35.00/0

Besides this scientific interest, trapped modes are significant for offshore engineering applications because of the "near-trapping phenomenon" discovered by Maniar & Newman (1997). They have found that for a long array of bottom-mounted cylinders, resonant modes occur as "near-trapping", and large diffraction forces are excited on the cylinders. The mechanism of such a resonant phenomenon has been explained by the present authors in connection with the Dirichlet trapped modes for an array of cylinders aligned perpendicular to the walls in a wave channel (Utsunomiya & Eatock Taylor 1998, 1999). The Dirichlet trapped mode, introduced by Maniar & Newman (1997), is a trapped mode where the Dirichlet boundary condition is applied on the channel walls. Although such a wave channel is nonphysical, the connection with near-trapping phenomena has been demonstrated by Maniar & Newman (1997) and by Utsunomiya & Eatock Taylor (1998, 1999).

Similar effects have been observed in Rayleigh–Bloch waves travelling along an infinite array of cylinders, and the essential equivalency between the Rayleigh–Bloch waves and the trapped modes in a wave channel has been demonstrated very recently (Porter & Evans 1999). Near-trapping modes have also been obtained for circular arrays of bottom mounted cylinders by Evans & Porter (1997).

On the other hand, the trapping phenomenon also affects radiation forces. Newman (1998) has examined the added mass and hydrodynamic damping of the "McIver toroid", and a large fluctuation of added mass over a relatively broad range of frequencies has been demonstrated. A similar observation has been made before by Linton & Evans (1992) for a vertical cylinder placed in a channel, although they did not place great emphasis on this phenomenon. Similar behaviour should also be obtained for an array of cylinders at the trapped-mode frequencies; that is, the radiation forces will also indicate singular behaviour, as well as the diffraction forces. This is the motivation for our examining the radiation problem for an array of cylinders.

We consider in this paper an array of elastically connected cylinders in a wave channel. The cylinders are surface-piercing and extend to the sea-bottom. They constitute an array in a line, and each cylinder is allowed to oscillate only in the direction parallel to the line.

For the single-cylinder case, the cut-off wavenumber (under which no radiation of wave energy to the ends of the channel is possible) is known to be $k = \pi/2d$, where d is the half-width of the channel. In the frequency range below the cut-off, the velocity potential becomes real-valued, and thus the resulting radiation force acting on the cylinder can be represented only by an added mass force. If the cylinder is allowed to oscillate only in the direction perpendicular to the channel walls, the system will have a pure-resonant mode.

However, for an array of cylinders, the usual application of the multipole expansion method leads to complex-valued potentials, and thus the radiation force will be represented by both added mass and hydrodynamic damping forces. In such a case, it may seem that the elastically connected cylinder arrays have no pure-resonant modes because of the energy dissipation due to radiation of waves to infinity. However, using the same technique as presented by Utsunomiya & Eatock Taylor (1999), we find that we can work with real-valued velocity potentials which radiate no wave energy to the ends of the channel for an equally spaced array of cylinders. Combining this idea with the modal analysis technique, in which we employ "dry-modes" of the periodic mass–spring system as modal functions, we have obtained real-valued radiation potentials, or only added mass forces as the radiation forces. The corresponding elastically connected cylinder array, therefore, has pure-resonant modes. Trapped modes for the corresponding diffraction problem are obtained as the limiting case when the stiffness of the springs has an infinite value.

2. FORMULATION

2.1. Statement of the Problem

Cartesian coordinates (x, y, z) are chosen such that the xy-plane is located on the mean free surface and the z-axis points upwards. The fluid is contained in a channel, the walls of which are located at $|y| = d$ and $|x| < \infty$, with the fluid depth being h. The N circular cylinders having the same radius a and extending vertically throughout the fluid domain are located along a perpendicular plane to the channel walls. The distances between the centres of the adjacent cylinders are taken to be $2s$ and the distances between the channel walls and the centres of cylinders at both ends of the row are s. Thus the half channel width d is equal to Ns. The (x, y) coordinates of the axis of each cylinder are represented by $(0, y_j)$, where

$$y_j = -d + (2j-1)s, \quad j = 1, 2, \ldots, N, \tag{1}$$

and N polar coordinates (r_j, θ_j) are defined with their origins at $(0, y_j)$ such that

$$x = r_j \cos\theta_j, \quad y - y_j = r_j \sin\theta_j, \quad j = 1, 2, \ldots, N. \tag{2}$$

Figure 1 illustrates the geometrical notation for the three cylinder case ($N = 3$).

The fluid is assumed to be inviscid and incompressible, and its motion to be time harmonic with angular frequency ω. Further, irrotational fluid motion is assumed so that a velocity potential $\Phi(x, y, z, t)$ exists. Thus,

$$\Phi(x, y, z, t) = \mathrm{Re}\{\phi(x, y, z)\mathrm{e}^{-\mathrm{i}\omega t}\}, \tag{3}$$

where $\phi(x, y, z)$ is a complex potential and t is time.

We apply separation of variables in order to factor out z-dependence, so that the following boundary conditions must be satisfied:

$$\frac{\partial\phi(x, y, z)}{\partial z} = \frac{\omega^2}{g}\phi(x, y, z) \quad \text{on } z = 0, \tag{4}$$

$$\frac{\partial\phi(x, y, z)}{\partial z} = 0 \quad \text{on } z = -h, \tag{5}$$

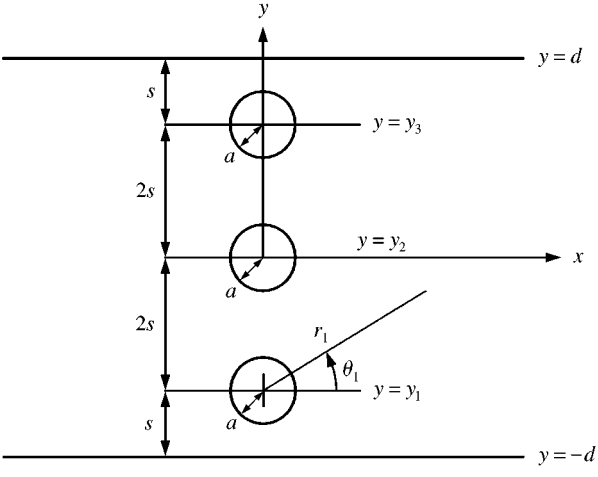

Figure 1. Geometrical notation of the problem for the three cylinder case ($N = 3$).

where g is the acceleration due to gravity. Then, the potential $\phi(x, y, z)$ can be represented as

$$\phi(x, y, z) = \sum_{l=0}^{\infty} f_l(z)\phi_l(x, y), \tag{6}$$

where the depth dependent eigenfunctions are

$$f_l(z) = M_l^{-1/2}\cos[k_l(z + h)], \tag{7}$$

$$M_l = (1 + \sin(2k_l h)/2k_l h)/2, \tag{8}$$

and k_l satisfies

$$k_l \tan k_l h + \omega^2/g = 0. \tag{9}$$

Here $k_l, l \geq 1$ are real and positive, while $k_0 = \mathrm{i}k$, k real and positive. The functions $f_l(z)$ satisfy the orthogonality relations

$$\frac{1}{h}\int_{-h}^{0} f_l(z) f_m(z)\,\mathrm{d}z = \delta_{lm}. \tag{10}$$

After using separation of variables, we can define the following boundary value problem for waves due to the oscillating cylinders, the velocities of which are defined as $\mathrm{Re}\{\dot{v}_j\,\mathrm{e}^{-\mathrm{i}\omega t}\}$ in the y-direction:

$$(\nabla^2 - k_l^2)\phi_l(x, y) = 0 \quad \text{in } |y| < d, r_j > a, \tag{11}$$

$$\frac{\partial \phi_l(x, y)}{\partial y} = 0 \quad \text{on } |y| = d, |x| < \infty, \tag{12}$$

$$\frac{\partial \phi_l(x, y)}{\partial x} = 0 \quad \text{on } x = 0, |y| < d, |y - y_j| > a, \tag{13}$$

$$\phi_l(x, y) \to 0 \quad \text{as } |x| \to \infty, |y| \leq d, \tag{14}$$

$$\frac{\partial \phi(r_j, \theta_j, z)}{\partial r_j} = \dot{v}_j \sin\theta_j \quad \text{on } r_j = a, -h < z < 0, \tag{15}$$

where $l = 0, 1, \ldots, \infty$, $j = 1, 2, \ldots, N$.

Multiplying both sides of equation (15) by $f_l(z)$ and integrating with respect to z from $-h$ to 0, it follows from relation (10) that the body boundary condition can be written as

$$\frac{\partial \phi_l(r_j, \theta_j)}{\partial r_j} = F_l \dot{v}_j \sin\theta_j \quad \text{on } r_j = a, \tag{16}$$

where

$$F_l = \frac{1}{h}\int_{-h}^{0} f_l(z)\,\mathrm{d}z = M_l^{-1/2}\sin(k_l h)/k_l h. \tag{17}$$

When Dirichlet boundary conditions are applied on the channel walls, equation (12) should be replaced by

$$\phi_l(x, y) = 0, \quad \text{on } |y| = d, |x| < \infty. \tag{18}$$

2.2. Multipole Expansions

The boundary value problem is defined for each of the potentials $\phi_l(x, y)$, thus it can be solved separately for each l. In order to solve the boundary value problem for $\phi_l(x, y)$,

$l = 0, 1, \ldots, \infty$, we employ the multipole expansion method. The potential $\phi_l(x, y)$ can be expressed in the following form:

$$\phi_l(x, y) = a \sum_{j=1}^{N} \sum_{n=0}^{\infty} (A^j_{2n;l} Z_{2n;l} \phi^j_{2n;l} + B^j_{2n+1;l} Z_{2n+1;l} \psi^j_{2n+1;l}), \tag{19}$$

where $A^j_{2n;l}$ and $B^j_{2n+1;l}$ are the unknown coefficients to be determined, and $\phi^j_{2n;l}$ and $\psi^j_{2n+1;l}$ are the channel multipoles [see McIver & Bennett (1993), Linton & McIver (1996)]. The factor $Z_{n;l}$ is defined as

$$\begin{aligned} Z_{n;l} &= \mathrm{J}'_n(ka)/\mathrm{Y}'_n(ka) \quad \text{for } l = 0, \\ &= \mathrm{I}'_n(k_l a)/\mathrm{K}'_n(k_l a) \quad \text{for } l = 1, 2, \ldots, \infty, \end{aligned} \tag{20}$$

where J_n and Y_n are the Bessel functions of the first and second kind of order n, respectively, and I_n and K_n are the modified Bessel functions of the first and second kind of order n, respectively.

The channel multipoles can be expressed as

$$\begin{aligned} \phi^j_{2n;l} &= \tilde{\mathrm{Y}}_{2n}(k_l r_j)\cos(2n\theta_j) \\ &\quad + \sum_{m=0}^{\infty} \{\alpha^j_{2n,2m;l} \tilde{\mathrm{J}}_{2m}(k_l r_j)\cos(2m\theta_j) + \beta^j_{2n,2m+1;l} \tilde{\mathrm{J}}_{2m+1}(k_l r_j)\sin[(2m+1)\theta_j]\}, \end{aligned} \tag{21}$$

$$\begin{aligned} \psi^j_{2n+1;l} &= \tilde{\mathrm{Y}}_{2n+1}(k_l r_j)\sin[(2n+1)\theta_j] \\ &\quad + \sum_{m=0}^{\infty} \{a^j_{2n+1,2m;l} \tilde{\mathrm{J}}_{2m}(k_l r_j)\cos(2m\theta_j) + b^j_{2n+1,2m+1;l} \tilde{\mathrm{J}}_{2m+1}(k_l r_j)\sin[(2m+1)\theta_j]\}, \end{aligned} \tag{22}$$

where

$$\begin{aligned} \tilde{\mathrm{Y}}_n(k_l r_j) &= \mathrm{Y}_n(kr_j) \quad \text{for } l = 0, \\ &= \mathrm{K}_n(k_l r_j) \quad \text{for } l = 1, 2, \ldots, \infty, \end{aligned} \tag{23}$$

$$\begin{aligned} \tilde{\mathrm{J}}_n(k_l r_j) &= \mathrm{J}_n(kr_j) \quad \text{for } l = 0, \\ &= \mathrm{I}_n(k_l r_j) \quad \text{for } l = 1, 2, \ldots, \infty. \end{aligned} \tag{24}$$

The coefficients are given in Utsunomiya & Eatock Taylor (1999) for $l = 0$, and they are given below for $l = 1, 2, \ldots, \infty$ as $\alpha^j_{2n,2m;l} = \alpha^{jj}_{2n,2m;l}$, etc.

Alternative expressions of the channel multipoles, where the singularity at $(0, y_j)$ is expanded about another point $(0, y_p)$, $j \neq p$, can be obtained from equations (A.10)–(A.15) of Linton & McIver (1996) for $l = 0$ and applying a similar procedure for $l = 1, 2, \ldots, \infty$, we obtain

$$\begin{aligned} \phi^j_{2n;l} &= \sum_{m=0}^{\infty} \{(C^{jp}_{2n,2m;l} + \alpha^{jp}_{2n,2m;l}) \tilde{\mathrm{J}}_{2m}(k_l r_p)\cos(2m\theta_p) \\ &\quad + (D^{jp}_{2n,2m+1;l} + \beta^{jp}_{2n,2m+1;l}) \tilde{\mathrm{J}}_{2m+1}(k_l r_p)\sin[(2m+1)\theta_p]\}, \end{aligned} \tag{25}$$

$$\begin{aligned} \psi^j_{2n+1;l} &= \sum_{m=0}^{\infty} \{(E^{jp}_{2n+1,2m;l} + a^{jp}_{2n+1,2m;l}) \tilde{\mathrm{J}}_{2m}(k_l r_p)\cos(2m\theta_p) \\ &\quad + (F^{jp}_{2n+1,2m+1;l} + b^{jp}_{2n+1,2m+1;l}) \tilde{\mathrm{J}}_{2m+1}(k_l r_p)\sin[(2m+1)\theta_p]\} \end{aligned} \tag{26}$$

with

$$C^{jp}_{2n,\,2m;\,l} = \frac{\varepsilon_m}{2}[\,(-1)^{m+n}\tilde{\Upsilon}_{2n+2m}(k_l R_{jp}) + (-1)^{m-n}\tilde{\Upsilon}_{2n-2m}(k_l R_{jp})], \tag{27}$$

$$D^{jp}_{2n,\,2m+1;\,l} = \pm\,[-(-1)^{m+n}\tilde{\Upsilon}_{2n+2m+1}(k_l R_{jp}) + (-1)^{m-n}\tilde{\Upsilon}_{2n-2m-1}(k_l R_{jp})], \tag{28}$$

$$E^{jp}_{2n+1,\,2m;\,l} = \pm\frac{\varepsilon_m}{2}[(-1)^{m+n}\tilde{\Upsilon}_{2n+2m+1}(k_l R_{jp}) + (-1)^{m-n}\tilde{\Upsilon}_{2n-2m+1}(k_l R_{jp})], \tag{29}$$

$$F^{jp}_{2n+1,\,2m+1;\,l} = -(-1)^{m+n}\tilde{\Upsilon}_{2n+2m+2}(k_l R_{jp}) + (-1)^{m-n}\tilde{\Upsilon}_{2n-2m}(k_l R_{jp}), \tag{30}$$

where $R_{jp} = 2s|j-p|$ and the plus sign of $\pm$ should be taken when $j < p$ and the minus sign of $\pm$ should be taken when $j > p$; $\varepsilon_m = 1$ for $m = 0$ and $\varepsilon_m = 2$ for $m \geq 1$.

Also, the following coefficients for $l \geq 1$ have been derived:

$$\alpha^{jp}_{2n,\,2m;\,l} = \varepsilon_m(-1)^{m+n} \int_0^\infty \frac{e^{-2k_l td}\cosh[k_l t(y_p - y_j)] \pm \cosh[k_l t(y_p + y_j)]}{\sinh(2k_l td)}\cosh(2nv)\cosh(2mv)\,dv, \tag{31}$$

$$\beta^{jp}_{2n,\,2m+1;\,l} = 2(-1)^{m+n} \int_0^\infty \frac{e^{-2k_l td}\sinh[k_l t(y_p - y_j)] \pm \sinh[k_l t(y_p + y_j)]}{\sinh(2k_l td)}\cosh(2nv)\cosh[(2m+1)v]\,dv, \tag{32}$$

$$a^{jp}_{2n+1,\,2m;\,l} = \varepsilon_m(-1)^{m+n} \int_0^\infty \frac{-e^{-2k_l td}\sinh[k_l t(y_p - y_j)] \pm \sinh[k_l t(y_p + y_j)]}{\sinh(2k_l td)}\cosh[(2n+1)v]\cosh(2mv)\,dv, \tag{33}$$

$$b^{jp}_{2n+1,\,2m+1;\,l} = 2(-1)^{m+n} \int_0^\infty \frac{-e^{-2k_l td}\cosh[k_l t(y_p - y_j)] \pm \cosh[k_l t(y_p + y_j)]}{\sinh(2k_l td)} \times \cosh[(2n+1)v]\cosh[(2m+1)v]\,dv, \tag{34}$$

where the plus sign of $\pm$ corresponds to the Neumann boundary conditions on the channel walls and the minus sign of $\pm$ to the Dirichlet boundary conditions, and $t = \cosh v$.

In order to evaluate integrals (31)–(34), the following formula has been utilized [1.331 in Gradshteyn & Ryzhik (1994)]:

$$\cosh nx = \sum_{k=0}^{[n/2]} \binom{n}{2k} \sinh^{2k} x \cosh^{n-2k} x. \tag{35}$$

Then the integrals have been numerically calculated for $\gamma = \sinh v$ from $\gamma = 0$ to ∞ with $t = (1+\gamma^2)^{1/2}$ by using NAG "d01amf" subroutine, where a relative error of 10^{-12} is specified as a tolerance limit.

Inserting the above multipoles given by equations (21)–(26) into equation (19), we can obtain the following expression for the total potential $\phi(r_p, \theta_p)$ in terms of the local polar coordinates (r_p, θ_p), $p = 1, 2, \ldots, N$, which is valid only in the vicinity of the cylinder p (the

restriction arising from use of Graf's addition theorem in the derivation of equations (25) and (26)):

$$\phi_l(r_p, \theta_p) = a \sum_{m=0}^{\infty} \{\tilde{A}^p_{2m;l} \tilde{\mathrm{Y}}_{2m}(k_l r_p)\cos(2m\theta_p) + \tilde{B}^p_{2m+1;l} \tilde{\mathrm{Y}}_{2m+1}(k_l r_p)\sin[(2m+1)\theta_p]$$
$$+ \sum_{j=1}^{N} \sum_{n=0}^{\infty} [\tilde{A}^j_{2n;l}(\tilde{\alpha}^{jp}_{2n,2m;l} \tilde{\mathrm{J}}_{2m}(k_l r_p)\cos(2m\theta_p) + \tilde{\beta}^{jp}_{2n,2m+1;l} \tilde{\mathrm{J}}_{2m+1}(k_l r_p)$$
$$\times \sin[(2m+1)\theta_p]) + \tilde{B}^j_{2n+1;l}(\tilde{a}^{jp}_{2n+1,2m;l} \tilde{\mathrm{J}}_{2m}(k_l r_p)\cos(2m\theta_p)$$
$$+ \tilde{b}^{jp}_{2n+1,2m+1;l} \tilde{\mathrm{J}}_{2m+1}(k_l r_p)\sin[(2m+1)\theta_p])]\}. \tag{36}$$

Here

$$\tilde{A}^j_{2n;l} = Z_{2n;l} A^j_{2n;l}, \qquad \tilde{B}^j_{2n+1;l} = Z_{2n+1;l} B^j_{2n+1;l}, \tag{37}$$

and

$$\tilde{\alpha}^{jp}_{2n,2m;l} = C^{jp}_{2n,2m;l} + \alpha^{jp}_{2n,2m;l} \quad \text{for } j \neq p,$$
$$= \alpha^{j}_{2n,2m;l} \quad \text{for } j = p, \tag{38}$$

are used for convenience. The coefficients $\tilde{\beta}^{jp}_{2n,2m+1;l}$, $\tilde{a}^{jp}_{2n+1,2m;l}$ and $\tilde{b}^{jp}_{2n+1,2m+1;l}$ are similarly defined as above.

Applying the boundary condition given by equation (16) on each of the cylinder surfaces, $p = 1, 2, \ldots, N$, we finally obtain the following systems of equations:

$$A^p_{2m;l} + \sum_{j=1}^{N} \sum_{n=0}^{\infty} (\tilde{A}^j_{2n;l} \tilde{\alpha}^{jp}_{2n,2m;l} + \tilde{B}^j_{2n+1;l} \tilde{a}^{jp}_{2n+1,2m;l}) = 0, \tag{39}$$

$$B^p_{2m+1;l} + \sum_{j=1}^{N} \sum_{n=0}^{\infty} (\tilde{A}^j_{2n;l} \tilde{\beta}^{jp}_{2n,2m+1;l} + \tilde{B}^j_{2n+1;l} \tilde{b}^{jp}_{2n+1,2m+1;l})$$
$$= \dot{v}_p F_l \delta_{m0}/ka \mathrm{J}'_1(ka) \quad \text{for } l = 0,$$
$$= \dot{v}_p F_l \delta_{m0}/k_l a \mathrm{I}'_1(k_l a) \quad \text{for } l \geq 1, \tag{40}$$

where $p = 1, 2, \ldots, N$, $m = 0, 1, \ldots, \infty$, and $l = 0, 1, \ldots, \infty$ in both cases. In the numerical calculations, the infinite systems must be truncated in terms of the Fourier modes, n and m: the total number of Fourier modes is taken as N_F for both odd and even modes. Furthermore, the infinite set of linear equations must be reduced to a finite set of equations. The total number of evanescent modes is thus defined by N_E such that $l = 0, 1, \ldots, N_E$.

We then introduce the following relationships:

$$A^{j(q)}_{2n;l} = A^{(q)}_{2n;l}(2/N)^{1/2}\cos[(2j-1)q\pi/2N] \quad \text{for } q = 1, 2, \ldots, N, \tag{41}$$

$$B^{j(q)}_{2n+1;l} = B^{(q)}_{2n+1;l}(2/N)^{1/2}\sin[(2j-1)q\pi/2N] \quad \text{for } q = 1, 2, \ldots, N-1, \tag{42}$$
$$= B^{(q)}_{2n+1;l}(1/N)^{1/2}\sin[(2j-1)q\pi/2N] \quad \text{for } q = N. \tag{43}$$

By introducing the above formulae, we can cancel out the propagating wave components, which are radiated from each multipole and do not vanish at large $|x|$, when $k < q\pi/2d$. We can then satisfy the boundary condition specified by equation (14). The rigorous proof of the above argument can be found in Utsunomiya & Eatock Taylor (1999).

At the same time, we express the complex displacement and velocity of the cylinders, v_j and $\dot{v}_j$, in terms of the following modal coordinates:

$$v_j = \sum_{q=1}^{N} \xi_q u_j^{(q)}, \tag{44}$$

$$\dot{v}_j = \sum_{q=1}^{N} \dot{\xi}_q u_j^{(q)}, \tag{45}$$

where $u_j^{(q)}$ is defined as

$$u_j^{(q)} = (2/N)^{1/2} \sin[(2j-1)q\pi/2N] \quad \text{for } q = 1, 2, \ldots, N-1, \tag{46}$$

$$= (1/N)^{1/2} \sin[(2j-1)q\pi/2N] \quad \text{for } q = N. \tag{47}$$

Here, the functions $u_j^{(q)}$ satisfy the orthogonality relations:

$$\sum_{j=1}^{N} u_j^{(q)} u_j^{(s)} = 0 \quad \text{for } q \neq s,$$

$$= 1 \quad \text{for } q = s. \tag{48}$$

We then determine the coefficients $A_{2m;l}^{(q)}$ and $B_{2m+1;l}^{(q)}$ for unit-amplitude velocity in the modal coordinate $\dot{\xi}_q$. Substituting equations (41)–(43), (46) and (47), and the relationship $\dot{v}_j = u_j^{(q)}$, into equations (39) and (40), and then summing up the equations after multiplying by similar modal functions to those in equations (41)–(43), we obtain

$$A_{2m;l}^{(q)} + \frac{2}{N} \sum_{n=0}^{N_F-1} \left[\tilde{A}_{2n;l}^{(q)} \sum_{p=1}^{N} \sum_{j=1}^{N} \cos\frac{(2j-1)q\pi}{2N} \cos\frac{(2p-1)q\pi}{2N} \tilde{\alpha}_{2n,2m;l}^{jp} + \tilde{B}_{2n+1;l}^{(q)} \sum_{p=1}^{N} \sum_{j=1}^{N} \sin\frac{(2j-1)q\pi}{2N} \cos\frac{(2p-1)q\pi}{2N} \tilde{a}_{2n+1,2m;l}^{jp} \right] = 0, \tag{49}$$

$$B_{2m+1;l}^{(q)} + \frac{2}{N} \sum_{n=0}^{N_F-1} \left[\tilde{A}_{2n;l}^{(q)} \sum_{p=1}^{N} \sum_{j=1}^{N} \cos\frac{(2j-1)q\pi}{2N} \sin\frac{(2p-1)q\pi}{2N} \tilde{\beta}_{2n,2m+1;l}^{jp} + \tilde{B}_{2n+1;l}^{(q)} \sum_{p=1}^{N} \sum_{j=1}^{N} \sin\frac{(2j-1)q\pi}{2N} \sin\frac{(2p-1)q\pi}{2N} \tilde{b}_{2n+1,2m+1;l}^{jp} \right]$$

$$= F_l \delta_{m0} / ka \mathrm{J}_1'(ka) \quad \text{for } l = 0,$$

$$= F_l \delta_{m0} / k_l a \mathrm{I}_1'(k_l a) \quad \text{for } l \geq 1, \tag{50}$$

where $m = 0, 1, \ldots, N_F - 1$, $l = 0, 1, \ldots, N_E$ and $q = 1, 2, \ldots, N-1$ in both equations. For the case of $q = N$, the above equations are simplified to

$$A_{2m;l}^{(q)} = 0, \tag{51}$$

$$B_{2m+1;l}^{(q)} + \frac{1}{N} \sum_{n=0}^{N_F-1} \left[\tilde{B}_{2n+1;l}^{(q)} \sum_{p=1}^{N} \sum_{j=1}^{N} \sin\frac{(2j-1)q\pi}{2N} \sin\frac{(2p-1)q\pi}{2N} \tilde{b}_{2n+1,2m+1;l}^{jp} \right]$$

$$= F_l \delta_{m0} / ka \mathrm{J}_1'(ka) \quad \text{for } l = 0,$$

$$= F_l \delta_{m0} / k_l a \mathrm{I}_1'(k_l a) \quad \text{for } l \geq 1. \tag{52}$$

By solving the above simultaneous linear equations, we can obtain the coefficients $A_{2n;l}^{(q)}$ and $B_{2n+1;l}^{(q)}$; thus we obtain the total potential from equation (19). Because all of the coefficients in the system matrix are real, the solutions of $A_{2n;l}^{(q)}$ and $B_{2n+1;l}^{(q)}$ also become real. It is to be

noted that the corresponding homogeneous systems of equations, where right-hand sides of equations (49)–(52) for $l = 0$ are set to be zero, determine trapped-mode solutions as their nontrivial solutions. Trapped-mode solutions around an array of cylinders have been obtained in such a way by Utsunomiya & Eatock Taylor (1999) in the context of the diffraction problem.

2.3. Added Mass

Substituting back equations (39) and (40) into equation (36), and applying the following Wronskian relationships for the Bessel functions (Linton & Evans 1990)

$$\mathrm{J}'_n(z)\mathrm{Y}_n(z) - \mathrm{Y}'_n(z)\mathrm{J}_n(z) = -2/\pi z, \tag{53}$$

$$\mathrm{I}'_n(z)\mathrm{K}_n(z) - \mathrm{K}'_n(z)\mathrm{I}_n(z) = 1/z, \tag{54}$$

we obtain the following simple expressions for the potential $\phi_l(r_p, \theta_p)_{r_p=a}$:

$$\phi_l(r_p, \theta_p)_{r_p=a} = \sum_{m=0}^{N_F-1} \left\{ \frac{1}{k\mathrm{J}'_{2m}(ka)} \left(-\frac{2}{\pi} \tilde{A}^p_{2m;l} \right) \cos(2m\theta_p) + \frac{1}{k\mathrm{J}'_{2m+1}(ka)} \left(-\frac{2}{\pi} \tilde{B}^p_{2m+1;l} + \dot{v}_p F_l \delta_{m0} \mathrm{J}_{2m+1}(ka) \right) \sin[(2m+1)\theta_p] \right\}$$

$$\text{for } l = 0, \tag{55}$$

$$\phi_l(r_p, \theta_p)_{r_p=a} = \sum_{m=0}^{N_F-1} \left\{ \frac{1}{k_l \mathrm{I}'_{2m}(k_l a)} \tilde{A}^p_{2m;l} \cos(2m\theta_p) + \frac{1}{k_l \mathrm{I}'_{2m+1}(k_l a)} (\tilde{B}^p_{2m+1;l} + \dot{v}_p F_l \delta_{m0} \mathrm{I}_{2m+1}(k_l a)) \sin[(2m+1)\theta_p] \right\} \quad \text{for } l \geq 1. \tag{56}$$

It should be noted that the above radiation potentials are real.

The total potential can thus be expressed by

$$\phi(r_p, \theta_p, z)_{r_p=a} = \sum_{q=1}^{N} \xi_q \sum_{l=0}^{N_E} f_l(z) \phi_l^{(q)}(r_p, \theta_p)_{r_p=a}, \tag{57}$$

where $\phi_l^{(q)}$ designates expressions (55) and (56) wherein expressions (41)–(43) are introduced. The added mass force induced on each cylinder is

$$F_j = \omega^2 \,\mathrm{Re}\left\{ \sum_{q=1}^{N} \xi_q \tilde{\lambda}^q_j \mathrm{e}^{-\mathrm{i}\omega t} \right\}, \tag{58}$$

where

$$\tilde{\lambda}^q_j = -\rho a \sum_{l=0}^{N_E} \int_{-h}^{0} f_l(z)\,\mathrm{d}z \int_0^{2\pi} \phi_l^{(q)}(r_j, \theta_j)_{r_j=a} \sin\theta_j \,\mathrm{d}\theta_j$$

$$= -\rho\pi a^2 h u_j^{(q)} \left[\frac{F_0}{ka\mathrm{J}'_1(ka)} \left(F_0 \mathrm{J}_1(ka) - \frac{2}{\pi} \tilde{B}^{(q)}_{1;0} \right) + \sum_{l=1}^{N_E} \frac{F_l}{k_l a \mathrm{I}'_1(k_l a)} (F_l \mathrm{I}_1(k_l a) + \tilde{B}^{(q)}_{1;l}) \right]. \tag{59}$$

The generalized added mass in terms of the modal coordinates ξ_q can then be obtained as

$$\tilde{\lambda}^{qs} = \sum_{j=1}^{N} u_j^{(q)} \tilde{\lambda}_j^s$$
$$= -\rho\pi a^2 h \left[\frac{F_0}{kaJ_1'(ka)} (F_0 J_1(ka) - \frac{2}{\pi} \tilde{B}_{1;0}^{(q)}) + \sum_{l=1}^{N_E} \frac{F_l}{k_l a I_1'(k_l a)} (F_l I_1(k_l a) + \tilde{B}_{1;l}^{(q)}) \right] \delta_{qs}. \tag{60}$$

Thus, the generalized added mass in terms of the modal coordinates becomes a diagonal matrix. The above expression is consistent with equation (3.46) of Linton & Evans (1992) for the single-cylinder case.

2.4. Resonant Modes for an Elastically Connected Cylinder Array

We connect adjacent cylinders by a spring whose spring constant is $K/4$, and the cylinder at the ends of the array and the adjacent wall are connected by a spring of stiffness $K/2$. We also assume that each cylinder has the same mass $M = \rho_b \pi a^2 h$. Using the method of Faulkner & Hong (1985), we obtain eigenfrequencies and eigenmodes (normal modes) of the dry system as

$$\omega_q^2 = \frac{K}{M} \frac{1 - \cos(q\pi/N)}{2}, \tag{61}$$
$$u_j^{(q)} = (2/N)^{1/2} \sin[(2j-1)q\pi/2N] \quad \text{for } q = 1, 2, \ldots, N-1,$$
$$= (1/N)^{1/2} \sin[(2j-1)q\pi/2N] \quad \text{for } q = N.$$

The above "dry-modes" have already been defined in equations (46) and (47), and used as the base coordinates for the generalized added mass. Therefore, the equations of motion in terms of the modal coordinates can be decoupled as

$$\{-\omega^2(M + \tilde{\lambda}^{qq}) + M\omega_q^2\} \xi_q = 0, \quad q = 1, 2, \ldots, N. \tag{62}$$

The eigenfrequencies for the full-system including the added-mass effect can thus be obtained from

$$-\omega^2(1 + (\rho/\rho_b)\lambda^{qq}) + \omega_q^2 = 0, \tag{63}$$

where $\lambda^{qq} = \tilde{\lambda}^{qq}/\rho\pi a^2 h$. The above equation can be rewritten as

$$\lambda^{qq} = \gamma_b \left(\frac{\omega_q^2}{\omega^2} - 1 \right) \tag{64}$$

or

$$\lambda^{qq} = \gamma_b \left(\frac{\omega_q^2 s}{g} \frac{1}{ks \tanh kh} - 1 \right), \tag{65}$$

where $\gamma_b = \rho_b/\rho$ is the relative density of the cylinders. The resonant frequency ω (or the corresponding wavenumber k) can thus be obtained schematically as a crossing point of the two graphs for λ^{qq} and the right-hand side of the above equations.

3. RESULTS AND DISCUSSION

Table 1 shows the convergence in terms of the truncation parameters, N_E and N_F, for the added mass coefficient λ^{11}. For both cases, (a) and (b), $N_F = 4$ and $N_E = 4$ give satisfactorily

TABLE 1

The added mass coefficient λ^{11} for the single cylinder in a channel. (a) $ks = 1{\cdot}0$, $a/s = 0{\cdot}5$, $h/s = 1{\cdot}0$, and (b) $ks = 1{\cdot}390$, $a/s = 0{\cdot}5$, $h/s = 1{\cdot}0$

N_E	$N_F = 1$	$N_F = 2$	$N_F = 4$	$N_F = 8$
(a)				
0	2·00800	2·00866	2·00867	2·00867
1	2·01649	2·01716	2·01716	2·01716
2	2·01671	2·01738	2·01738	2·01738
4	2·01675	2·01741	2·01742	2·01742
8	2·01675	2·01742	2·01742	2·01742
(b)				
0	349·54902	350·17397	350·26314	350·26314
1	349·57658	350·20153	350·29070	350·29070
2	349·57718	350·20213	350·29130	350·29130
4	349·57727	350·20223	350·29139	350·29140
8	349·57728	350·20224	350·29140	350·29141

convergent results. We thus employ $N_F = 4$ and $N_E = 4$ in the following calculations, unless specified explicitly. It should be noted from Table 1(b) that the singular behaviour of the added mass around the trapped-mode wavenumber ($ks = 1{\cdot}391314$ for this case) is due to the singular behaviour of the propagating wave component, and the evanescent modes do not contribute to the singular behaviour.

Figures 2–4 show the added mass coefficient λ^{11} and the determination of the resonant-mode wavenumbers based on equation (65). As indicated by the solid lines, the added mass coefficients exhibit singular behaviour around the trapped-mode wavenumber ($ks = 1{\cdot}391314$ for the Neumann channel; and $ks = 3{\cdot}071722$ for the Dirichlet channel) as has already been shown by Linton & Evans (1992) for the single cylinder in a channel. The

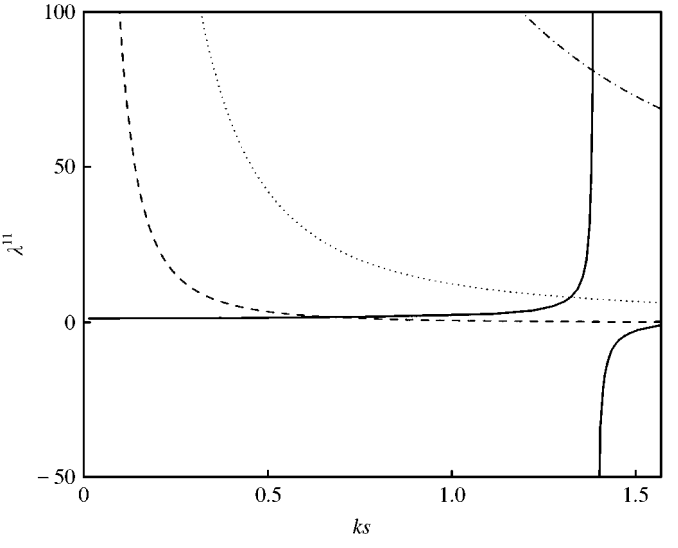

Figure 2. The added mass coefficient λ^{11} for the single cylinder in a channel with Neumann boundary conditions when $h/s = 1{\cdot}0$ and $a/s = 0{\cdot}5$ (——). The other lines are the right-hand side of equation (65) for $\gamma_b = 1{\cdot}0$ and $\omega_1^2 s/g = 1{\cdot}0$ (– – –); $\omega_1^2 s/g = 10{\cdot}0$ (····); and $\omega_1^2 s/g = 100{\cdot}0$ (–·–·–).

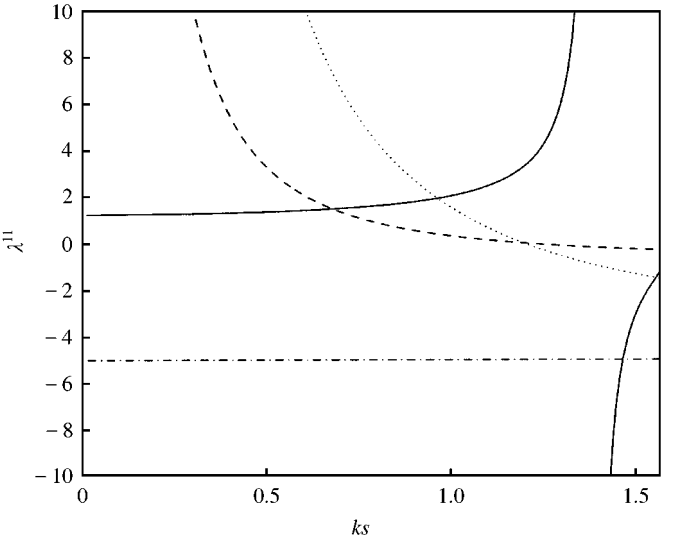

Figure 3. The added mass coefficient λ^{11} for the single cylinder in a channel with Neumann boundary conditions when $h/s = 1{\cdot}0$ and $a/s = 0{\cdot}5$ (——). The other lines are the right-hand side of equation (65) for $\gamma_b = 1{\cdot}0$ and $\omega_1^2 s/g = 1{\cdot}0$ (– – –); $\gamma_b = 5{\cdot}0$ and $\omega_1^2 s/g = 1{\cdot}0$ (····); and $\gamma_b = 5{\cdot}0$ and $\omega_1^2 s/g = 0{\cdot}0$ (–·–·–).

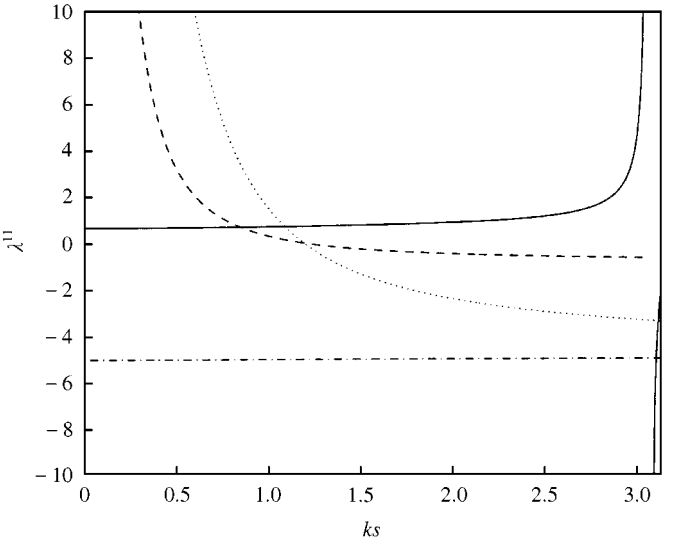

Figure 4. The added mass coefficient λ^{11} for the single cylinder in a channel with Dirichlet boundary conditions when $h/s = 1{\cdot}0$ and $a/s = 0{\cdot}5$ (——). The other lines are the right-hand side of equation (65) for $\gamma_b = 1{\cdot}0$ and $\omega_1^2 s/g = 1{\cdot}0$ (– – –); $\gamma_b = 5{\cdot}0$ and $\omega_1^2 s/g = 1{\cdot}0$ (····); and $\gamma_b = 5{\cdot}0$ and $\omega_1^2 s/g = 0{\cdot}0$ (–·–·–).

lines for the right-hand side of equation (65) for several parameters are also drawn in the same figures, and the crossing points with the solid line correspond to the resonant-mode wavenumbers. The resonant-mode frequency ω can be obtained from the dispersion relation.

As the stiffness of the springs becomes large, the resonant-mode wavenumber approaches the trapped-mode wavenumber, as shown in Figure 2. A pure-resonant mode will be

observed for the system without springs, as shown in Figure 3, where the graph for $\gamma_b = 5{\cdot}0$ and $\omega_1^2 s/g = 0{\cdot}0$ crosses the solid line in the negative added-mass region. It is obvious that as the relative density becomes large for the system without springs, resonant-mode wavenumbers approach the trapped-mode wavenumber. For some combination of parameters, multiple resonant states may occur as shown in Figure 3, where the dotted line crosses the solid line both in the positive and negative added-mass regions. For the case of Dirichlet boundary conditions on the channel walls (Figure 4), the cut-off wavenumber becomes π/s; however the qualitative character is essentially the same as for the Neumann boundary conditions case (Figure 3).

Resonant-mode wavenumbers are shown in Tables 2 and 3 for arrays of cylinders in a channel with Neumann and Dirichlet boundary conditions, respectively. In order to check

TABLE 2

Resonant-mode wavenumber ks for elastically connected cylinder arrays in a channel with Neumann boundary conditions; $a/s = 0{\cdot}5$, $h/s = 1{\cdot}0$ and $\gamma_b = 1{\cdot}0$. Calculated for $N_F = N_E = 8$ ($N_F = N_E = 4$)

N	q	$\omega_N^2 s/g = 1$	$\omega_N^2 s/g = 10$	$\omega_N^2 s/g = 100$	$\omega_N^2 s/g = 1000$	Trapped-mode
1	1	0·681994	1·323659	1·385567	1·390748	1·391313
		(0·681994)	(1·323659)	(1·385567)	(1·390748)	
2	1	0·491416	0·774612	0·779874	0·780239	0·780278
		(0·491416)	(0·774612)	(0·779874)	(0·780239)	
2	2	0·681998	1·323663	1·385568	1·390748	1·391313
		(0·681998)	(1·323663)	(1·385568)	(1·390748)	
4	1	0·275827	0·391518	0·392119	0·392160	0·392164
		(0·275827)	(0·391518)	(0·392119)	(0·392160)	
4	2	0·491416	0·774612	0·779874	0·780239	0·780278
		(0·491416)	(0·774612)	(0·779874)	(0·780239)	
4	3	0·632481	1·127222	1·150102	1·151753	1·151931
		(0·632481)	(1·127222)	(1·150102)	(1·151753)	
4	4	0·682000	1·323665	1·385568	1·390748	1·391313
		(0·682000)	(1·323665)	(1·385568)	(1·390748)	

TABLE 3

Resonant-mode wavenumber ks for elastically connected cylinder arrays in a channel with Dirichlet boundary conditions; $a/s = 0{\cdot}5$, $h/s = 1{\cdot}0$ and $\gamma_b = 1{\cdot}0$. Calculated for $N_F = N_E = 8$ ($N_F = N_E = 4$)

N	q	$\omega_N^2 s/g = 1$	$\omega_N^2 s/g = 10$	$\omega_N^2 s/g = 100$	$\omega_N^2 s/g = 1000$	Trapped-mode
1	1	0·853968	2·927808	3·064407	3·071030	3·071722
		(0·853968)	(2·927812)	(3·064407)	(3·071030)	
2	1	0·491417	0·774612	0·779874	0·780239	0·780278
		(0·491417)	(0·774612)	(0·779874)	(0·780239)	
2	2	0·853947	2·927402	3·064405	3·071030	3·071722
		(0·853947)	(2·927407)	(3·064405)	(3·071030)	
4	1	0·275827	0·391518	0·392119	0·392160	0·392164
		(0·275827)	(0·391518)	(0·392119)	(0·392160)	
4	2	0·491417	0·774612	0·779874	0·780239	0·780278
		(0·491417)	(0·774612)	(0·779874)	(0·780239)	
4	3	0·632484	1·127222	1·150102	1·151753	1·151931
		(0·632484)	(1·127222)	(1·150102)	(1·151753)	
4	4	0·853936	2·927191	3·064405	3·071030	3·071722
		(0·853937)	(2·927196)	(3·064405)	(3·071030)	

the convergence of the results, they have been calculated both for $N_F = N_E = 8$ and $N_F = N_E = 4$. As can be seen in Tables 2 and 3, all values are convergent with five figures accuracy, although most of them are convergent with six figures accuracy.

For the Dirichlet channel, the elastically connected array of cylinders must have free–free boundary conditions for the existence of pure resonant-modes; that is the springs at both ends have to be removed. At the same time, the modal coordinates used for the hydrodynamic problem must be consistent with the dry-modes for the free–free system (Utsunomiya & Eatock Taylor 1999).

As is obvious from Tables 2 and 3, as the stiffness of the springs becomes large, the resonant-mode wavenumbers approach the corresponding trapped-mode wavenumbers. For the same value of q/N, the same resonant-mode wavenumbers ks are obtained (with five figures accuracy). This can easily be recognized by considering symmetry; dry-modes for the periodic system and added-mass for the periodic array of cylinders both exhibit such symmetry. Equivalency of the added mass (or radiation potentials) for Neumann and Dirichlet channels is also observed for cases $q < N$; which is similar to the behaviour of the trapped-modes for arrays of cylinders in a channel (Utsunomiya & Eatock Taylor 1999; Porter & Evans 1999). Equipotential contours on the mean free surface ($z = 0$) for the single cylinder in a channel are shown in Figure 5. Global potential distributions at large $|x|$ are similar in (a) and (b); the potentials for both of them become exponentially small as $|x|$ approaches infinity. However, the potential distributions around the cylinder are different in (a) and (b). For the case of (a) where the wavenumber is much lower than the

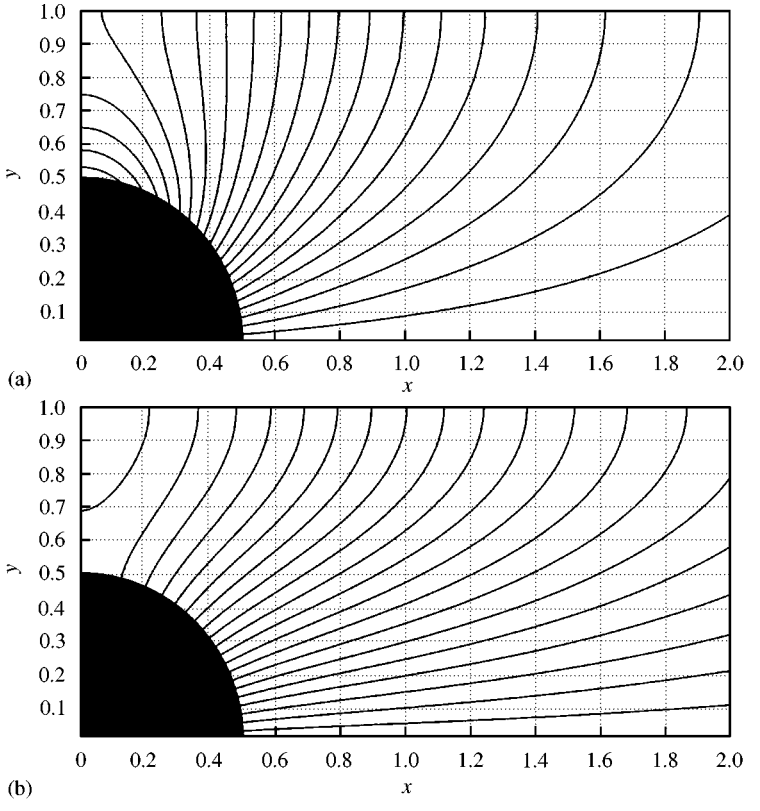

Figure 5. Equipotential contours on $z = 0$ for the single cylinder in a channel with Neumann boundary conditions when $a/s = 0{\cdot}5$ and $h/s = 1{\cdot}0$; (a) $ks = 0{\cdot}681994$; and (b) $ks = 1{\cdot}390748$.

trapped-mode wavenumber, the satisfaction of the boundary condition (15) is easily recognized; whereas for the case of (b) where the wavenumber is close to the trapped-mode wavenumber, the satisfaction of the boundary condition (15) is not obvious. This means that a small magnitude of oscillation of the cylinder can excite a large wave if the wavenumber is close to the trapped-mode wavenumber. It is also obvious that Figure 5(b) gives a similar equipotential contour to the trapped-mode, for which $\phi_n = 0$ is satisfied on the cylinder surface.

Equipotential contours on the mean free surface ($z = 0$) for four cylinders in a channel are shown in Figure 6. Due to the symmetry or anti-symmetry of the potentials with respect to the xz-plane and the symmetry with respect to the yz-plane, only one-quadrant of the full-plane is indicated. As is obvious from Figures 6(d) and 5(a), the case for $N = q = 4$ is equivalent to the case for $N = q = 1$. A similar observation can be made for $N = 2$, $q = 1$ and $N = 4$, $q = 2$ (the case of Figure 6(b)).

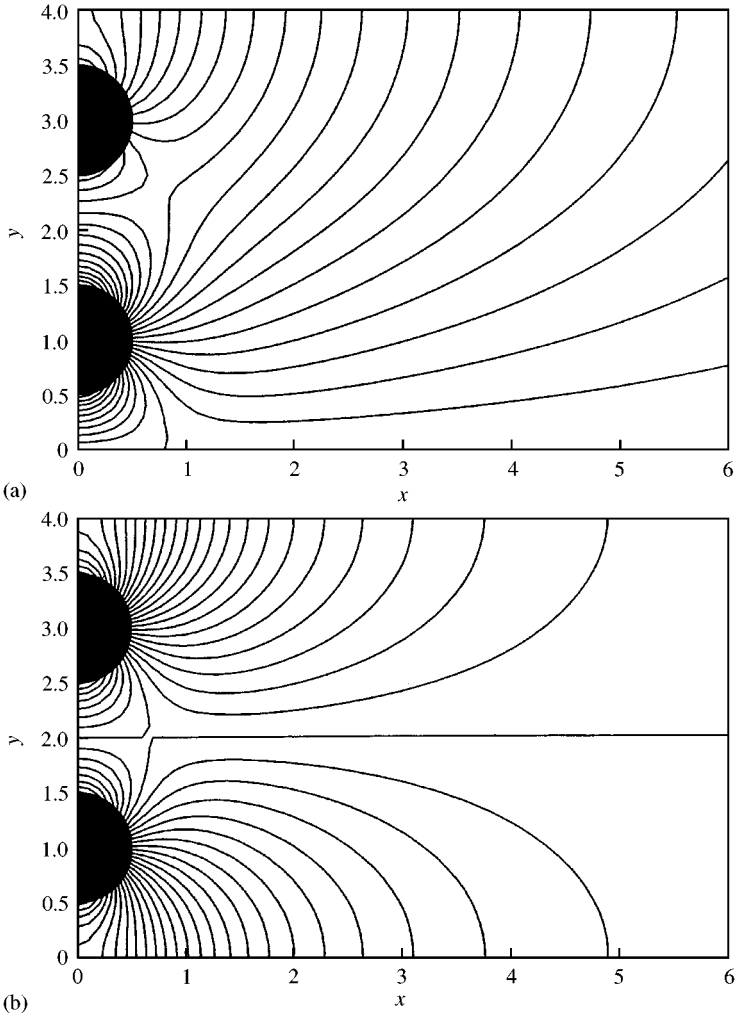

Figure 6. Equipotential contours on $z = 0$ for four cylinders in a channel with Neumann boundary conditions when $a/s = 0{\cdot}5$ and $h/s = 1{\cdot}0$: (a) $q = 1$, $ks = 0{\cdot}275827$; (b) $q = 2$, $ks = 0{\cdot}491416$; (c) $q = 3$, $ks = 0{\cdot}632481$; and (d) $q = 4$, $ks = 0{\cdot}682000$.

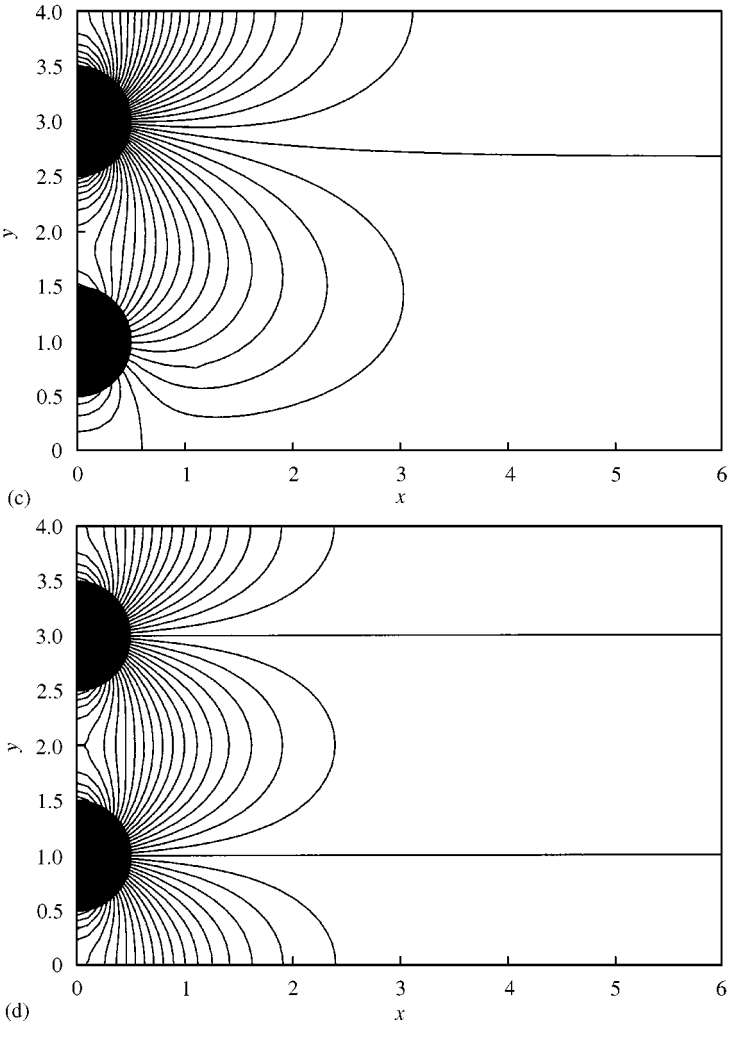

Figure 6. continued.

4. CONCLUSIONS

This paper has examined resonant-modes for an array of elastically connected cylinders aligned across a wave channel. Nonradiating wave modes for the array of cylinders oscillating in the direction along the line of the array have been found to exist below the channel cut-off wavenumbers. The multipole expansion method has been employed to demonstrate the existence of such nonradiating wave modes, and the technique used by Utsunomiya & Eatock Taylor (1999) for demonstrating trapped-modes for an array of cylinders in a channel has been applied here. The wet-modes for the periodic array of cylinders have been shown to have the same modal shapes as the corresponding dry-modes.

In this paper, we have restricted ourselves to the very limited cases where the arrays of cylinders have a periodic nature both in the hydrodynamic and mechanical sense; and we have succeeded to show the existence of pure-resonant modes for such periodic structures. If we remove such restrictions, e.g. when some cylinders have different radius, some springs have different spring constants or some cylinders have different mass, the demonstration of

pure-resonant modes seems impossible, since the system can no more be decoupled and thus the oscillation mode which radiates energy down the tank will be excited.

One might consider that pure resonant-modes demonstrated in this paper are very special cases, and no direct engineering application would be available. As shown by Maniar & Newman (1997), however, trapped-modes in a channel are directly related to the resonant phenomenon for diffraction around a finite long array of cylinders, which is relevant for engineering applications. This paper has demonstrated that such resonant phenomena will occur in some periodic hydro-elastic systems; we need thus to examine in future research the existence of resonant modes for systems having more realistic configurations, such as a floating airport supported by large number of arrays of truncated cylinders or a floating bridge spanning a wide channel.

ACKNOWLEDGEMENTS

T. Utsunomiya would like to acknowledge the support of the Kajima foundation during his one-year visit to the University of Oxford.

References

Callan, M., Linton, C. M. & Evans, D. V. 1991 Trapped modes in two-dimensional wave-guides. *Journal of Fluid Mechanics* **229,** 51–64.

Evans, D. V. & Kuznetsov, N. 1998 Trapped modes. In *Gravity Waves in Water of Finite Depth* (ed. J. N. Hunt), pp. 127–168. Southampton: Computational Mechanics.

Evans, D. V. & Porter, R. 1997 Near-trapping of waves by circular arrays of vertical cylinders. *Applied Ocean Research* **19,** 83–99.

Faulkner, M. & Hong, D. P. 1985 Free vibrations of a mono-coupled periodic system. *Journal of Sound and Vibration* **99,** 29–42.

Gradshteyn, I. S. & Ryzhik, I. M. 1994 *Tables of Integrals, Series, and Products*, 5th edition. London: Academic Press.

Linton, C. M. & Evans, D. V. 1990 The interaction of waves with arrays of vertical circular cylinders. *Journal of Fluid Mechanics* **215,** 549–569.

Linton, C. M. & Evans, D. V. 1992 The radiation and scattering of surface waves by a vertical circular cylinder in a channel. *Philosophical Transactions of the Royal Society of London* **A338,** 325–357.

Linton, C. M. & McIver, P. 1996 The scattering of water waves by an array of circular cylinders in a channel. *Journal of Engineering Mathematics* **30,** 661–682.

Maniar, H. D. & Newman, J. N. 1997 Wave diffraction by a long array of cylinders. *Journal of Fluid Mechanics* **339,** 309–330.

McIver, P. & Bennett, G. S. 1993 Scattering of water waves by axisymmetric bodies in a channel. *Journal of Engineering Mathematics* **27,** 1–29.

Newman, J. N. 1998 Hydrodynamic analysis of the McIver toroid. In 13*th International Workshop on Water Waves and Floating Bodies*, Alphen aan den Rijn, The Netherlands.

Porter, R. & Evans, D. V. 1999 Rayleigh–Bloch surface waves along periodic gratings and their connection with trapped modes in waveguides. *Journal of Fluid Mechanics* **386,** 233–258.

Ursell, F. 1951 Trapping modes in the theory of surface waves. *Proceedings of the Cambridge Philosophical Society* **47,** 347–358.

Utsunomiya, T. & Eatock Taylor, R. 1998 Analogies for resonances in wave diffraction problems. In 13*th International Workshop on Water Waves and Floating Bodies*, Alphen aan den Rijn, The Netherlands.

Utsunomiya, T. & Eatock Taylor, R. 1999 Trapped modes around a row of circular cylinders in a channel. *Journal of Fluid Mechanics* **386,** 259–279.